7-1-2004

Micromagnetic Domain Structures in Cylindrical Nickel Dots

George D. Skidmore
University of Minnesota, Minneapolis

Andrew Kunz
Marquette University, andrew.kunz@marquette.edu

C. E. Campbell
University of Minnesota, Minneapolis

E. Dan Dahlberg
University of Minnesota, Minneapolis

Published version. *Physical Review B,* Vol. 70, No. 1 (July 2004). DOI.

Micromagnetic domain structures in cylindrical nickel dots

George D. Skidmore,* Andrew Kunz,† C. E. Campbell, and E. Dan. Dahlberg
Magnetic Microscopy Center, School of Physics and Astronomy, University of Minnesota, Minneapolis, Minnesota 55455, USA
(Received 11 November 2003; published 29 July 2004)

The magnetic domain structures of cylindrical nickel dots (diameters from 40 nm to 1700 nm) with anisotropy parallel to the cylinder axis is predicted by the ratio of the dot diameter to the stripe period of unpatterned films with the same perpendicular anisotropy. The dominant domain structure for a given ratio increases in complexity as the ratio increases. We present evidence for the full micromagnetic domain structure for the simplest cases.

DOI: 10.1103/PhysRevB.70.012410 PACS number(s): 75.50.Tt, 75.60.Ch, 75.70.Kw, 75.75.+a

The ability to create and measure properties of nanoelements with uniform size and shape and the availability of increasing computational power has led to an explosion of experimental and computational studies involving magnetic particle arrays[1–17] impacting fundamental magnetism research and technological applications. Current experimental understanding of domain structure and reversal mechanisms in magnetic nanoelements typically comes from the collective or average behavior of the many elements in fabricated arrays.[2–5] Recent simulations have furthered this understanding in the case of structures primarily consisting of single domains with in-plane magnetization.[4–7]

In this paper we present a study of the magnetic domain states observed in perpendicularly magnetized cylindrical magnetic dots, a significant advancement over previous studies.[8–13] Utilizing high-resolution magnetic force microscopy (MFM) (Ref. 18) and three-dimensional micromagnetics calculations, we have studied the size evolution of the micromagnetic structure in individual nickel dots. In particular, it is most important to note that the excellent agreement between the simulations and the MFM images provides a high level of confidence that the simulations accurately describe the micromagnetic structure at length scales beyond the MFM resolution, and reveal the underlying three-dimensional domain structure that is not available experimentally. The metastable domain states described below, impact dynamical studies[14–17] in that the specific micromagnetic structures determine the phase space available for reversal.

We find an excellent predictor of the magnetic structure of our nickel dots to be the ratio of the diameter of the dots to the period of the magnetic stripes[19,20] which form in unpatterned films of the same height. We define this simple dimensionless ratio to be the micromagnetic characterization parameter D_0, given by

$$D_0 = d/\lambda, \tag{1}$$

where d is the cylinder diameter and λ is the repeat period of the film stripe pattern. The stripe period found in thin films is dependent on many material parameters and also is a function of the thickness of the film.[19] Previous work on cobalt nanosquares has also shown a domain state dependence on thickness.[10,13] We find that the stability of the magnetic structures is determined by the magnetic energies found both in the bulk and in films of the same thickness, as well as the size and geometry of the dots.

Our experimental study not only includes a study of Ni dot thicknesses ranging from 48 nm to 140 nm, but also expands previous work[10,13] by exploring dot diameters ranging from 40 to 1700 nm. The results were qualitatively the same for all thicknesses, but here we will report only the most complete study, that of the 100 nm thick dots with diameters in the range of 60 to 1000 nm. The parameter D_0 is valid for the entire range of cylindrical dots studied.

The unpatterned films of this thickness had a stripe period λ of approximately 200 nm. The stripe period was found to be robust for all diameter dots observed. The cylindrical dots, well separated to minimize any effect of interactions, were made by thermally evaporating nickel through a lithographically defined mask.[21] Simultaneously grown films were used to determine the perpendicular magnetic anisotropy $K_u = 6\times10^5$ erg/cm^3 and the stripe domain period.[22] A commercially available MFM,[23] supplemented with fabricated high-resolution MFM tips, provided approximately 30 nm resolution with minimal sample perturbation.[18] To further ensure that there was no significant tip field induced perturbation of the magnetic state, MFM images were always taken twice on a dot with the same tip with opposite tip magnetizations so that both north pole [Figs. 1(a,d) and Figs. 2(a,d,g)] and south pole [Figs. 1(b,e) and Figs. 2(b,e,h)] tip magnetizations were used.[24] The right-hand columns of Figs. 1 and 2 corresponds to the simulated z component of the magnetization of the cylindrical dots.

The dots were simulated[25] numerically using the Landau-Lifshitz-Gilbert (LLG) equation.[26] The LLG equation describes the precessional motion for the magnetic moments $\mathbf{m}_i$ comprising the cylinder.[27] We simulate the dots with identical cubic elements at each site i. The LLG equation is given by

$$\frac{d\mathbf{m}_i}{dt} = \frac{-\gamma}{1+\alpha^2}\mathbf{m}_i\times\mathbf{H}_i - \frac{\alpha\gamma}{(1+\alpha^2)M_s}\mathbf{m}_i\times(\mathbf{m}_i\times\mathbf{H}_i), \tag{2}$$

where the effective magnetic field $\mathbf{H}_i$ at site i is the sum of three effective fields: dipole fields, exchange fields with neighboring grains, and the perpendicular uniaxial anisotropy field found experimentally. The magnetic moment M_s and exchange coupling of the cubic elements are appropriate for bulk nickel.[28] Since the LLG method is deterministic,

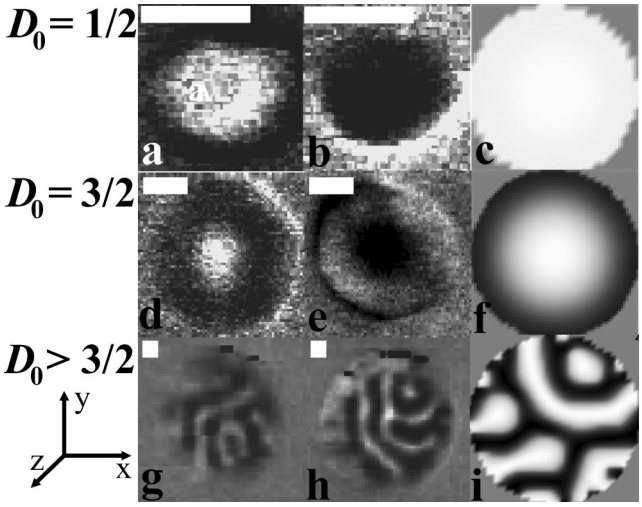

FIG. 1. MFM (a,b,d,e,g,h) and simulated (c,f,i) images of the z component of the magnetization for ring domains in nickel dots with increasing diameter from top to bottom. The MFM images in (a,b) and (d–e) are taken on the same dot with opposite tip magnetization (Ref. 24). D_0 is the ratio of the dot diameter to the thin-film stripe period. The scale bars represent 100 nm.

various random magnetic initial states were used to determine the different final stable states in a single sample. All magnetic structures obtained in this manner were also observed experimentally.

The figures have been sorted in terms of the observed dichotomy of ring (Fig. 1) and stripe (Fig. 2) domains. There it is seen that the dots with smallest diameters [Figs. 1(a–f) and 2] have rather simple domain structures, while at diameters where D_0 is larger than 3/2 [Figs. 1(g–i)] the nickel dots begin to take on a complex stripe domain structure with

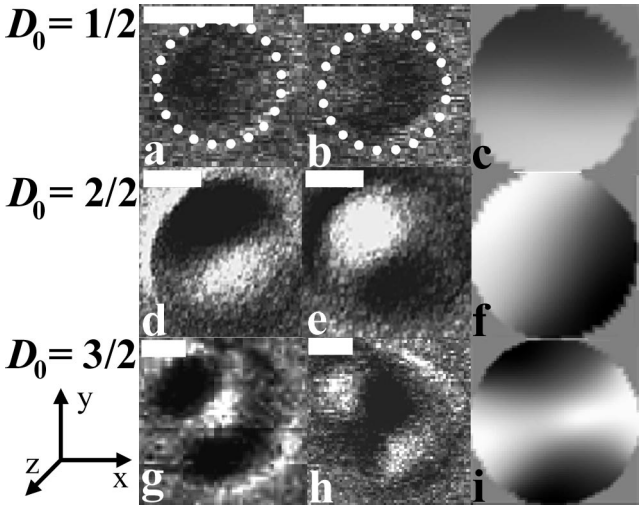

FIG. 2. MFM (a,b,d,e,g,h) and simulated (c,f,i) images of the z component of the magnetization for stripe domains in nickel dots. The MFM images in (a,b,d,e,g,h) are taken on the same dot with opposite tip magnetization (Ref. 24). D_0 is the ratio of the dots diameter to the thin film stripe period. At the smallest diameters (a–c) the dot is almost invisible to the MFM as the magnetic flux is enclosed within the dot. The scale bars represent 100 nm.

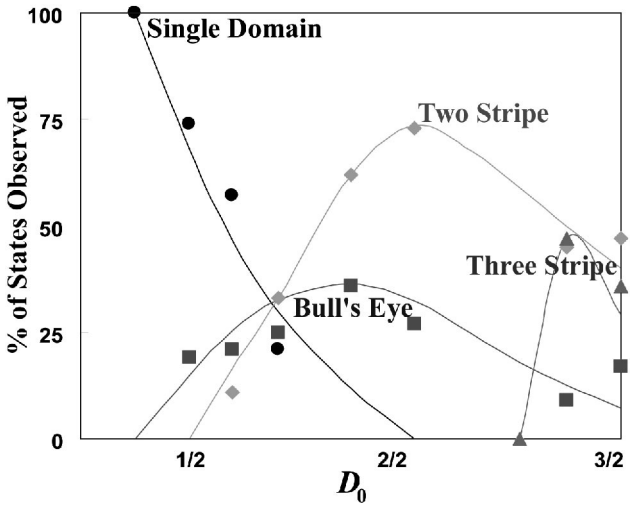

FIG. 3. Experimentally observed ratio of domain state abundances. At the smallest diameters only the single-domain state exists. As the diameter grows, more complicated domain structures appear. Past $D_0 = 1/2$, more than one magnetic state is available in dots of the same size.

somewhat random patterns (but constrained by the nearly constant stripe period). Figure 3 summarizes the distribution of the domain structures for all of the approximately 3000 dots investigated experimentally, representing 37 different diameter dots of 100 nm thickness. It is apparent in Fig. 3 that more than one magnetic state can be found in dots of the same diameter. It is also true that different domain patterns are often found in the same dot after applying saturating magnetic fields, leading to the conclusion that slight differences in the dots do not stabilize one magnetic structure over another. In the following we discuss the results for specific D_0 ratios.

Only one stable structure appears in the smallest dots, $D_0 < 1/2$, a single-domain flower shown in Figs. 1(a–c), and in y-z cross section in Fig. 4(a). The strong contrast between the oppositely magnetized tip [Fig. 1(a,b)] agrees with the simulation result shown in Fig. 4(a) where the top surface of the dot is shown to be an open domain. At dot diameters less than $D_0 = 1/2$ the flower state is found to have the lowest energy density and no other stable magnetic structure is found in either the simulations or experiments. Figure 3 shows the dominance of the flower state for the smaller values of D_0.

The onset of a second stable state is found beginning near $D_0 = 1/2$ as shown in Fig. 3. This state exhibits very little contrast when viewed with MFM, as seen in Figs. 2(a,b). As can be seen in the y-z cross section in Fig. 4(b), this state is essentially a domain wall or vortex in that the magnetic moments are radially oriented around a vortex line aligned along the x axis of the dot.[29] This vortex structure makes these magnetic particles almost invisible in MFM; because of this complete flux closure, we refer to it as the in-plane vortex structure. As is faintly observed in Figs. 2(a,b), there is some field leakage along the edges parallel to the vortex axis.

As the diameter of the dot is increased there is an evolu-

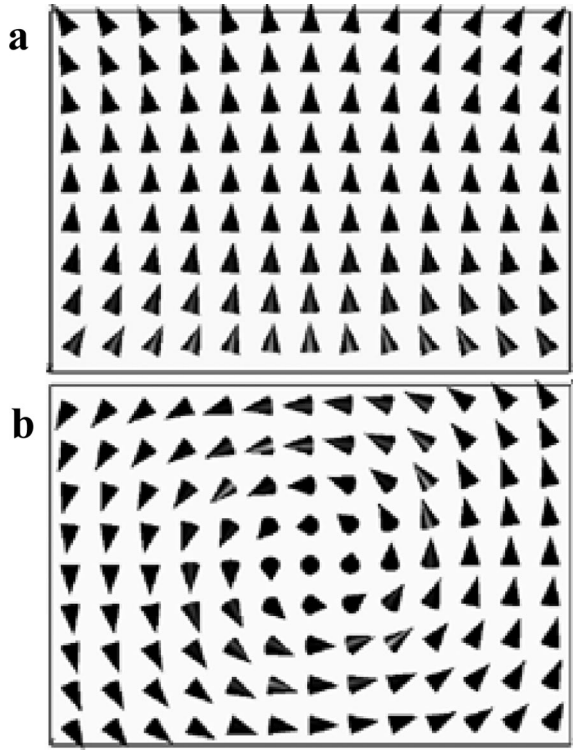

FIG. 4. (a) Flower (open magnetization) and (b) vortex (closed magnetization) cross sections showing the direction of the magnetic moments. The circulation of the magnetic domains about the *x* axis in (b) shows complete magnetic flux closure and explains why the vortex state is nearly invisible to the MFM.

tion into two-domain states as illustrated in Figs. 2(d–f). Comparing Figs. 2(a–c) with Figs. 2(d–f), it is seen that the in-plane vortex structure has evolved into a domain wall separating an up domain from a down domain, or a two-stripe structure. The MFM image of those two domains is now quite distinct. Also, the strong contrast between the oppositely aligned tip [Figs. 2(d,e)] shows the magnetization should be pointing strongly out of the top surface.[24] As might be expected, this is the most frequently seen structure near $D_0=1$, where the diameter equals the period of the film stripe pattern.

Similarly as the D_0 increases towards unity the single-domain flower state evolves into a bull's-eye structure. This structure consists of an upwardly magnetized domain separated from a downward domain by a circular domain wall. This domain wall closes on itself, minimizing the magnetic flux and thus the magnetostatic energy. Experimentally, we observe weak contrast in the outer domain and strong contrast in the central domain when the probing tip is reversed [Figs. 1(d,e)].[24] The simulations show this is because the state consists of an open central domain, and an outer domain with a more closed structure.

A three-stripe domain structure, shown in Figs. 2(g,h), is seen in the MFM experiments and simulations starting at diameters near $D_0=3/2$. These three-stripe patterns show a strong MFM signal above every domain, and obvious contrast when the tip is reversed, indicating magnetic moments pointing out of (or into) the top surface, in agreement with the simulations.[24] This three-stripe structure is an obvious step from the two-stripe structure described above.

Figures 1(g,h) are images of near-micron-sized dots taken with only one-tip magnetization, while Fig. 1(i) is a simulated domain structure at the same diameter. The large diameter dots allow for many domains, and many different stable structures consisting of stripes (straight and curved) and rings. At $D_0>3/2$, the number of available states becomes too great to classify. However, we find that the stripes are of approximately the same width in the experiments and the simulations. Further, we find the domain walls prefer to terminate perpendicular to, or run parallel to, the edge of the dots. In this diameter range we also find stable multiring bull's-eye patterns, which appear to be the lowest energy structures at these sizes.

As we have shown, the bulk properties of the material and the geometry of the particles determine the micromagnetic states of the cylindrical nickel dots we have studied. It can be seen in Fig. 3 that D_0 $(=\mathrm{d}/\lambda)$ is an excellent predictor of the micromagnetic state. For all the particles investigated (all thicknesses in the entire range 48–140 nm), the states we observed are consistent with the stripe periods observed in the films.[17]

As a simple description of the evolution of the micromagnetics of these particles, we have outlined two convenient sequences: stripes and rings. The ring sequence starts with the smallest particles imaged, which exhibit only the flower structure. In the evolution of the ring structures, the flower state can be viewed as the center of the bull's-eyes which appear at larger diameters, first as a single-ring bull's-eye at diameters larger than $D_0=1$. The rings of the bull's eyes may be viewed as circular stripe domains. Of course rings are simply stripes that close on themselves.

The (linear) stripe sequence begins with the in-plane vortex—essentially a domain wall—at small diameters, which then grows into stripes as the diameter of the dots increases. Each approximate half-integer step in D_0 leads to the formation of an additional stripe.

In conclusion, we have shown that the full magnetic structure of nanoscale cylindrical magnetic dots may be determined by a combination of high-resolution MFM and micromagnetic simulations and that the ratio of the dot diameter to stripe period provides a simple predictor of the allowed microscopic domain structures. We find that the resultant magnetic structure of the nanoscale dots is a rich function of the size, ranging from single-domain flower structures at the smallest diameters to multidomain structures characterized by different in-plane vortex patterns.

A very interesting result of our investigation is the explosion of allowed states for $D_0>3/2$ after the rather small number of allowed states for smaller sized particles. Most important, since the simulations have no adjustable parameters, the agreement of the simulations with the MFM images provides confidence that the micromagnetic simulations accurately describe the micromagnetic state on a scale beyond the 30-nm resolution of the MFM.

We wish to acknowledge assistance or helpful discussions with Dr. Eric Granstrom, Dr. Jake Schmidt, and Dr. Christo-

pher Merton, as well as research support from the Office of Naval Research (Grant No. N00014-94-1-0123), the University of Minnesota MRSEC (Grant No. NSF/DMR-9809364), the University of Minnesota Graduate School, and the University of Minnesota Supercomputing Institute for Digital Simulation and Advanced Technology. Two of the authors (C.E.D. and E.D.D.) also thank the ONR (Grant No. Navy/N00014-02-1-0815) for their support of this work.

*Present address: Zyvex Corp., 1321 N. Plano Rd., Richardson, TX 75081, USA.

†Present address: Lawrence University, Appleton, WI 54912, USA.

[1] R.D. Gomez, T.V. Luu, A.O. Pak, K.J. Kirk, and J.N. Chapman, J. Appl. Phys. **85**, 6163 (1999).

[2] C.A. Ross, M. Hwang, H. Shima, J.Y. Cheng, M. Farhoud, T.A. Savas, N.J. Smith, W. Schwarzacher, F.M. Ross, M. Redjdal, and F.B. Humphrey, Phys. Rev. B **65**, 144417 (2002).

[3] R.P. Cowburn, A.O. Adeyeye, and M.E. Welland, Phys. Rev. Lett. **81**, 5414 (1998).

[4] R.P. Cowburn, D.K. Koltsor, A.O. Adeyeye, M.E. Welland, and D.M. Tricker, Phys. Rev. Lett. **83**, 1042 (1999).

[5] R.P. Cowburn, J. Phys. D **33**, R1 (2000).

[6] K.J. Kirk, S. McVitie, J.N. Chapman, and C.D.W. Wilkenson, J. Appl. Phys. **89**, 7174 (2001).

[7] J. Raabe, R. Pulwey, R. Sattler, T. Schweinbock, J. Zweck, and D. Weiss, J. Appl. Phys. **88**, 4437 (2000).

[8] G.J. Parker and C. Cerjan, J. Appl. Phys. **87**, 5514 (2000).

[9] T.C. Schulthess, M. Benakli, P.B. Visscher, K.D. Sorge, J.R. Thompson, F.A. Modine, T.E. Haynes, L.A. Boatner, G.M. Stocks, and W.H. Butler, J. Appl. Phys. **89**, 7594 (2001).

[10] M. Hehn, R. Ferre, K. Ounadjela, J.P. Bucher, and F. Rousseaux, J. Magn. Magn. Mater. **165**, 5 (1997).

[11] C. Haginoya, S. Heike, M. Ishibashi, K. Nakamura, K. Koike, T. Yoshimura, J. Yamanoto, and Y. Hirayama, J. Appl. Phys. **85**, 8327 (1999).

[12] C. Stamm, F. Marty, A. Vaterlaus, V. Weich, S. Egger, U. Maier, U. Ramsperger, H. Fuhrmann, and D. Pescia, Science **282**, 449 (1998).

[13] M. Hehn, K. Ounadjela, K.P. Bucher, F. Rousseaux, D. Decanini, B. Bartenlian, and C. Chappert, Science **272**, 1782 (1996).

[14] J. Rothman, M. Klaui, L. Lopez-Diaz, C.A.F. Vaz, A. Blecoh, J.A.C. Bland, Z. Cui, and R. Speaks, Phys. Rev. Lett. **86**, 1098 (2001).

[15] R.H. Koch, J.G. Deak, D.W. Abraham, P.L. Trouilloud, R.A. Altman, Y. Lu, W.J. Gallagher, R.E. Scheuerlein, K.P. Roche, and S.S.P. Parkin, Phys. Rev. Lett. **81**, 4512 (1998).

[16] R.L. Stamps and B. Hillebrands, Appl. Phys. Lett. **75**, 1143 (1999).

[17] N. Dao, S.L. Whittenburg, and R.P. Cowburn, J. Appl. Phys. **90**, 5235 (2001).

[18] G.D. Skidmore, and E.D. Dahlberg, Appl. Phys. Lett. **71**, 3293 (1997).

[19] M. Hehn, S. Padovani, K. Ounadjela, and J.P. Bucher, Phys. Rev. B **54**, 3428 (1996).

[20] S. Hameed, P. Talagala, R. Naik, L.E. Wenger, V.M. Naik, and R. Proksch, Phys. Rev. B **64**, 184406 (2001).

[21] S. A. Campbell, *The Science and Engineering of Microelectronic Fabrication* (Oxford Press, New York, 1996), pp. 206–214.

[22] Andrew Kunz, G.D. Skidmore, E.D. Dahlberg, and C.E. Campbell (unpublished).

[23] Digital Instruments, 112 Robin Hill Road, Santa Barbara, California 93119, USA.

[24] The main concern of tip-sample interactions is that the field from the tip produces irreversible changes in the domain state; this is proven to not be the case in the present study since the images with the two different tip magnetizations always find the same micromagnetic state. In general, attractive parts of the images are more pronounced than the repulsive parts as the average distance of the cantilever from the sample will be smaller or larger, respectively, and this accounts for the discrepancy in the images produced by the two different tip magnetizations. We also note that the MFM signal is dominated by open domains (where the magnetization points out of the surface of the dot) which is correlated with the micromagnetic simulations.

[25] Andrew Kunz, Ph.D. Thesis, University of Minnesota, 2000.

[26] LLG Inc., Tempe, AZ 85282, USA.

[27] E.D. Boerner and H.N. Bertram, IEEE Trans. Magn. **33**, 3052 (1997).

[28] C. Serberino and H.N. Bertram, IEEE Trans. Magn. **33**, 3055 (1997).

[29] W. Rave, K. Fabian, and A. Hubert, J. Magn. Magn. Mater. **190**, 332 (1998).